J. Fluid Mech. (1984), *vol.* 140, *pp.* 153–174
Printed in Great Britain

Temporal moments at large distances downstream of contaminant releases in rivers

By RONALD SMITH

Department of Applied Mathematics and Theoretical Physics, University of Cambridge, Silver Street, Cambridge CB3 9EW

(Received 15 July 1983)

This paper concerns the effects of topographic changes upon the dispersion of contaminants in rivers. Exact analytical results are derived for the time-of-arrival, temporal variance and skewness far downstream of a sudden contaminant release. It is demonstrated that there can exist optimal discharge sites, such that at all positions far downstream the maximum concentrations are minimized.

1. Temporal instead of longitudinal moments

Much work on contaminant dispersion in shear flows is based upon Aris' (1956) method of moments. This powerful method replaces the full advection–diffusion equation by a hierarchy of equations for successive longitudinal moments of the contaminant distribution. For most practical purposes an adequate description of the concentration can be obtained with just the first few longitudinal moments (e.g. the area, centroid and variance). An important aspect of Aris' (1956) work is that it gives a rigorous justification, at large times after discharge, for Taylor's (1953) heuristic approach to shear dispersion.

Although the flow can be time-dependent (Aris 1960), there is an intrinsic restriction in the method of moments that the flow must be longitudinally uniform. For varying channels there is coupling between all the longitudinal moments, and, unless the changes in the channel are very gradual, there is no meaningful hierarchy. The few theoretical calculations that have been attempted for flows that vary rapidly along their length (Fischer 1969; Smith 1983) have been heuristic, in the spirit of the work of Taylor (1953).

Tsai & Holley (1978) pointed out that moments with respect to time provide a tractable alternative to spatial moments for the theoretical study of contaminant dispersion. Given that longitudinal moments can be used even when the flow is time-dependent, it is natural to enquire whether temporal moments remain tractable when the flow is longitudinally non-uniform. The present paper shows that this is indeed the case. It is confirmed that at large distances downstream of a contaminant release, the upstream memory character of the dispersion process is exactly as inferred by the author (Smith 1983).

An important bonus of the method of calculation is that from the values of just two functions it is possible to compare the relative merits of all possible discharge sites. For straight channels the peak pollution level at a fixed monitoring position can always be improved by displacing the discharge site slightly further upstream (Smith 1981; Daish 1984). However, it is demonstrated in the final section of this paper that, when the channel varies markedly, there can exist optimal discharge sites which are better than all nearby sites upstream, downstream or across the flow. It

is only by a substantial upstream relocation of the discharge that the peak concentration level at the monitoring position can be further improved.

2. Moment equations and some notation

In a typical stream, with water depth much less than the channel breadth, Fischer (1967) showed that the shear dispersion associated with the lateral variations is greatly in excess of the vertical-shear dispersion coefficient. This in turn is an order of magnitude greater than the longitudinal turbulent eddy diffusivity (Elder 1959). Thus for simplicity we shall neglect longitudinal diffusion, average out the vertical structure, and take the advection–diffusion equation to have the form

$$m_1 m_2 h(\partial_t c + u_1 \partial_x c) - \partial_y\left(\frac{m_1}{m_2} h\kappa \partial_y c\right) = m_1 m_2 hq, \tag{2.1a}$$

with

$$h\kappa \partial_y c = 0 \quad \text{on} \quad y = y_L, y_R, \tag{2.1b}$$

and

$$\partial_x(m_1 m_2 h u_1) = 0. \tag{2.2}$$

Here (x, y) are curvilinear coordinates aligned along and across the flow (see figure 1), $m_1(x, y)$, $m_2(x, y)$ are metric coefficients, $c(x, y, t)$ is the contaminant concentration, $h(x, y)$ the water depth, $m_1 u_1(x, y)$ the depth-averaged flow velocity (u_1 is the rate of crossing of x-contours), $\kappa(x, y)$ the transverse dispersion coefficient, q the depth-averaged source strength, and y_L, y_R denote the left and right banks of the channel. In the absence of inflows or recirculation, the banks are streamlines, and so y_L, y_R are constants independent of x. The alignment of the x-coordinate with the flow ensures that there are no crossflow terms $v\partial_y c$.

It is the neat form of the advected rate of change $(\partial_t + u_1 \partial_x)$ that makes it convenient to denote the velocity by $m_1 u_1$. Similarly, an m_1 factor is included in the definition of area averages:

$$\bar{f} = \frac{\int_{y_R}^{y_L} m_1 m_2 hf \, dy}{\int_{y_R}^{y_L} m_1 m_2 h \, dy}. \tag{2.3}$$

Far downstream of the discharge the contaminant will have become well mixed across the stream and will be carried along at the area-averaged velocity $\bar{u}_1$. Thus to a first approximation the time of arrival at x of a contaminant released at $t = 0$, $x = x_0$ is

$$\tau(x) = \int_{x_0}^{x} \frac{dx'}{\bar{u}_1(x')}. \tag{2.4}$$

To suppress the occurrence of secularly growing terms, we define temporal moments $c^{(j)}(x, y)$ relative to this time displacement $\tau(x)$:

$$c^{(j)} = \int_{-\infty}^{\infty} (t - \tau)^j c(x, y, t) \, dt \quad (j = 0, 1, \ldots). \tag{2.5}$$

Successive temporal moments of the advection–diffusion equation (2.1) yield the hierarchy of equations

$$m_1 m_2 h u_1 \partial_x c^{(j)} - \partial_y\left(\frac{m_1}{m_2} h\kappa \partial_y c^{(j)}\right) = m_1 m_2 h q^{(j)} + j m_1 m_2 h\left(1 - \frac{u_1}{\bar{u}_1}\right) c^{(j-1)}, \tag{2.6a}$$

with

$$h\kappa\,\partial_y c^{(j)} = 0 \quad \text{on} \quad y = y_L, y_R. \tag{2.6b}$$

If we assume that the discharge has the form

$$q(y)\,\delta(x-x_0)\,\delta(t) \tag{2.7}$$

(i.e. a sudden release at $x = x_0$, $t = 0$ with cross-stream profile $q(y_0)$, then the

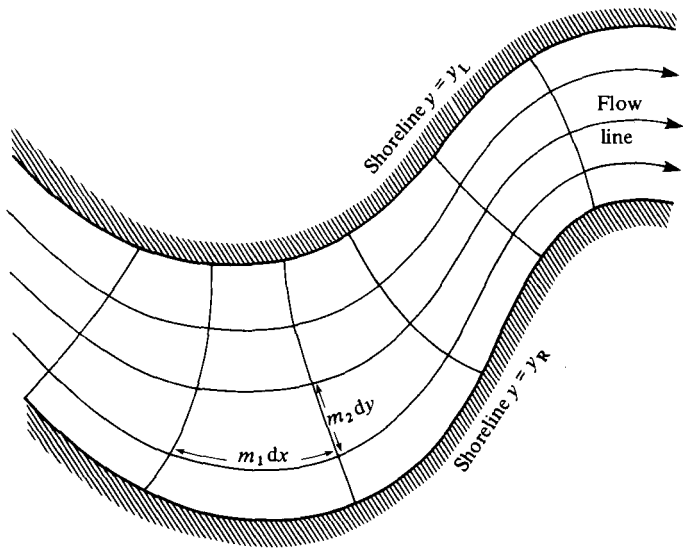

FIGURE 1. Flow-following coordinate system for a meandering channel.

occurrence of the $q^{(j)}$ forcing term on the right-hand side of (2.6*a*) can be replaced by the starting conditions (Tsai & Holley 1978, equation 20)

$$c^{(0)} = \frac{q}{u_1}, \quad c^{(1)} = c^{(2)} = \ldots = 0 \quad \text{at} \quad x = x_0. \tag{2.8}$$

The form of the x-derivative term in (2.6*a*) leads us to define the flux-weighted average

$$[f] = \frac{\int_{y_R}^{y_L} m_1 m_2 h u_1 f\,dy}{\int_{y_R}^{y_L} m_1 m_2 h u_1\,dy}. \tag{2.9}$$

If we make the decomposition

$$c^{(j)} = [c^{(j)}] + \Delta c^{(j)}, \tag{2.10}$$

then the area averages of the moment equations (2.6), (2.8) yield the useful sequels

$$[c^{(0)}] = \frac{\bar{q}}{\bar{u}_1}\bigg|_{x=x_0}, \tag{2.11}$$

$$[c^{(j)}] = j\int_{x_0}^{x} \frac{\Delta c^{(j-1)}}{\bar{u}_1}\,dx'. \tag{2.12}$$

3. The dosage

The zero moment $c^{(0)}(x, y)$ is the integrated total concentration experienced at the location (x, y). For contaminants with accumulative effects, this dosage is of importance in its own right. Here we regard $c^{(0)}$ as being only one item of information concerning the time evolution of the concentration at (x, y).

Using the notation (2.10) in (2.6), (2.8), we obtain the advection–diffusion equation

$$m_1 m_2 h u_1 \partial_x \Delta c^{(0)} - \partial_y \left(\frac{m_1}{m_2} h \kappa \partial_y \Delta c^{(0)} \right) = 0, \tag{3.1a}$$

with

$$h \kappa \partial_y \Delta c^{(0)} = 0 \quad \text{on} \quad y = y_L, y_R, \tag{3.1b}$$

and

$$\Delta c^{(0)} = \frac{\bar{u}_1 q - \bar{q} u_1}{u_1 \bar{u}_1} \quad \text{at} \quad x = x_0. \tag{3.1c}$$

There is zero net discharge associated with the starting conditions (3.1c). Thus, we can infer that at large distances downstream the effect of cross-stream diffusion will be to make $\Delta c^{(0)}$ smear out to zero, i.e. the dosage becomes uniform across the flow and independent of x. The transients decay exponentially fast on a diffusion lengthscale of order $\bar{u} B^2 / \kappa$.

The total volume of contaminant released into the flow is

$$Q = \int_{y_R}^{y_L} m_1 m_2 h q \, dy \Big|_{x = x_0}, \tag{3.2}$$

while the volume flux of water along the channel is given by

$$F = \int_{y_R}^{y_L} m_1 m_2 h u_1 \, dy \quad \text{independent of } x. \tag{3.3}$$

Thus the asymptotic value of the dosage can be written

$$c^{(0)} \sim [c^{(0)}] = \frac{Q}{F}. \tag{3.4}$$

This only depends on the volume of contaminant and the river flow rate, so is independent of either the discharge profile $q(y_0)$ or the discharge location x_0. Hence it is only by reducing Q that the dosages experienced far downstream can be ameliorated. By contrast, it is shown below that concentrations are functions of x, y, x_0 and $q(y_0)$ (i.e. the concentration depends upon the observation site, the discharge location and the detailed character of the discharge).

4. Time of arrival

Pursuing the analysis to the next temporal moment, we see from (2.12) with $j = 1$, that, rather than needing the full solution $\Delta c^{(0)}$ of (3.1a–c), it suffices that we can evaluate the integral

$$[c^{(1)}] = \int_{x_0}^{x} \frac{\overline{\Delta c^{(0)}}}{\bar{u}_1} \, dx'. \tag{4.1}$$

A general prescription for the evaluation of such integrals related to advection–diffusion equations is given in Appendix A. In the notation used in Appendix A this particular case corresponds to

$$a(x,y) = \Delta c^{(0)}, \quad M(x,y) = 0, \quad N(x,y) = 1. \tag{4.2}$$

Thus, following the general prescription, we are led to introduce an auxiliary function $b = G_-(x,y)$ which satisfies the upstream advection equation

$$-m_1 m_2 h u_1 \partial_x G_- - \partial_y\left(\frac{m_1}{m_2} h\kappa \partial_y G_-\right) = m_1 m_2 h\left(1-\frac{u_1}{\bar{u}_1}\right), \tag{4.3a}$$

with

$$h\kappa \partial_y G_- = 0 \quad \text{on} \quad y = y_L, y_R, \tag{4.3b}$$

and

$$[G_-] = 0. \tag{4.3c}$$

The conditions (A 6, A 7) needed to derive the reduction formula (A 8) are satisfied. Thus we have the result

$$[c^{(1)}] = [G_- \Delta c^{(0)}]_{x_0} - [G_- \Delta c^{(0)}] = \left(\frac{\overline{qG_-}}{\bar{u}_1}\right)_{x_0} - [G_- \Delta c^{(0)}]. \tag{4.4}$$

At large distances downstream of the discharge the last term tends to zero.

Relative to the mean travel time (2.4), the flux-averaged time of arrival of the contaminant at x can be defined as

$$[T] = \frac{[c^{(1)}]}{[c^{(0)}]} \sim \left(\frac{\overline{qG_-}}{\bar{q}}\right)_{x_0}. \tag{4.5}$$

Thus there is a tendency for a late arrival if the discharge profile $q(y_0)$ is weighted towards regions of positive G_-. From the right-hand-side forcing terms in (4.3a), we can infer that G_- is largest in the slowest-flowing part of the stream (see figure 2). Hence, in accord with physical intuition, releasing a contaminant in the slower-flowing part of the channel delays the arrival of the contaminant at locations far downstream.

To investigate the y-dependence of $c^{(1)}$, we again use the $\Delta c^{(j)}$ notation (2.10), and we consider the equation

$$\begin{aligned} &m_1 m_2 h u_1 \partial_x \Delta c^{(1)} - \partial_y\left(\frac{m_1}{m_2} h\kappa \partial_y \Delta c^{(1)}\right) \\ &\quad = m_1 m_2 h\left(1-\frac{u_1}{\bar{u}_1}\right)[c^{(0)}] + m_1 m_2 h\left(1-\frac{u_1}{\bar{u}_1}\right)\Delta c^{(0)} - m_1 m_2 h\overline{\Delta c^{(0)}}\left(\frac{u_1}{\bar{u}_1}\right), \end{aligned} \tag{4.6a}$$

with

$$h\kappa \partial_y \Delta c^{(1)} = 0 \quad \text{on} \quad y = y_L, y_R, \tag{4.6b}$$

and

$$\Delta c^{(1)} = 0 \quad \text{at} \quad x = x_0. \tag{4.6c}$$

At large distances downstream the $\Delta c^{(0)}$ forcing terms vanish. Thus we have the asymptote

$$\Delta c^{(1)} \sim [c^{(0)}] G_+, \tag{4.7}$$

where the auxiliary function $G_+(x,y)$ satisfies the downstream advection–diffusion equation

$$m_1 m_2 h u_1 \partial_x G_+ - \partial_y\left(\frac{m_1}{m_2} h\kappa \partial_y G_+\right) = m_1 m_2 h\left(1-\frac{u_1}{\bar{u}_1}\right), \tag{4.8a}$$

with

$$h\kappa\,\partial_y G_+ = 0 \quad \text{on} \quad y = y_{\mathrm{L}}, y_{\mathrm{R}}, \tag{4.8b}$$

and

$$[G_+] = 0. \tag{4.8c}$$

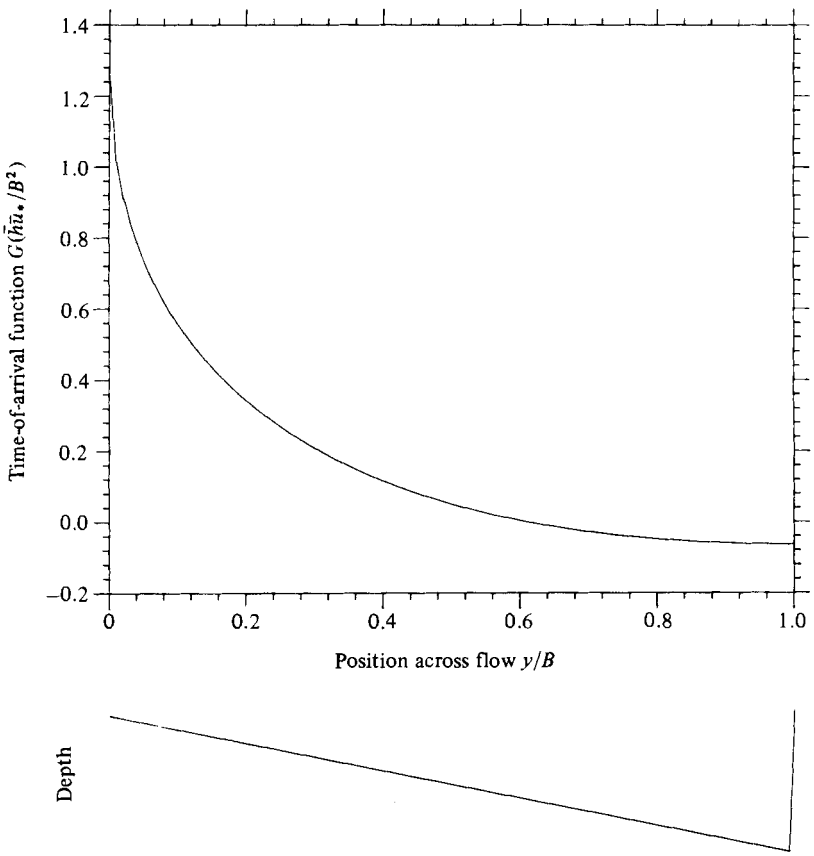

FIGURE 2. Time-of-arrival function $G_+ = G_-$ for a longitudinally uniform channel with a triangular depth profile.

The resulting asymptotic expression for the time of arrival (relative to the mean travel time (2.4)) is

$$T = \frac{c^{(1)}}{c^{(0)}} \sim \left(\frac{\overline{qG}_-}{\bar{q}}\right)_{x_0} + G_+(x, y). \tag{4.9}$$

As was the case with its upstream counterpart, G_+ tends to be positive where the flow rate is small. Thus again we have a physically obvious implication: that the contaminant arrives later for observation sites (x, y) in the slower-moving part of the flow.

For subsequent use we note that with

$$a(x, y) = G_+, \quad b(x, y) = G_-, \quad \text{i.e.} \quad M = N = 1, \tag{4.10}$$

the prescription given in Appendix A yields the result (A 8))

$$\int_{x_0}^{x} \frac{\bar{G}_+}{\bar{u}_1}\,\mathrm{d}x' = \int_{x_0}^{x} \frac{\bar{G}_-}{\bar{u}_1}\,\mathrm{d}x' + [G_+ G_-]_{x_0} - [G_+ G_-]. \tag{4.11}$$

5. Shear-dispersion coefficient

Substituting the asymptotic result (4.7) into (2.12) with $j = 2$, we have

$$[c^{(2)}] \sim 2[c^{(0)}] \int_{x_0}^{x} \frac{\bar{G}_+}{\bar{u}_1} \mathrm{d}x' + \text{constant}, \tag{5.1}$$

where the constant is associated with transient $\overline{\Delta c^{(1)}}$ contributions.

For the flux-averaged concentration distribution the temporal variance can be defined:

$$\Sigma_T^2 = \frac{[c^{(2)}]}{[c^{(0)}]} - \left(\frac{[c^{(1)}]}{[c^{(0)}]}\right)^2. \tag{5.2}$$

Thus at large distances downstream we infer from (4.5), (5.1) that

$$\Sigma_T^2 \sim 2 \int_{x_0}^{x} \frac{\bar{G}_+}{\bar{u}_1} \mathrm{d}x' + \text{constant}. \tag{5.3}$$

Making allowance for the disparity between spatial and temporal measures of the contaminant evolution, we can interpret (5.3) as defining the local shear-dispersion coefficient

$$D_{\mathrm{loc}} = \bar{u}_1^2 \bar{G}_+ \tag{5.4}$$

(Smith 1983, equation 6.4). The important features of this generalization of Taylor's (1953) classic result are that there is an upstream memory, and that D_{loc} can be negative, i.e. higher averaged concentrations can be experienced further downstream when there are marked flow changes (Fukuoka & Sayre 1973).

6. Influence of the discharge profile on the pollution level

For a longitudinally uniform channel, Smith (1981) and Daish (1984) have shown that the precise discharge distribution $q(y_0)$ can affect the concentrations over a substantial distance downstream of the discharge (i.e. several diffusion lengthscales). The implication is that the constants in equations (5.1), (5.3) can be quite large, and need to be evaluated.

Returning to (4.6*a–c*), we write

$$\Delta c^{(1)} = [c^{(0)}] G_+ + \delta c^{(1)}, \tag{6.1}$$

where the decaying contribution $\delta c^{(1)}$ satisfies the equation

$$m_1 m_2 h u_1 \partial_x \delta c^{(1)} - \partial_y \left(\frac{m_1}{m_2} h \kappa \partial_y \delta c^{(1)}\right) = m_1 m_2 h \left(1 - \frac{u_1}{\bar{u}_1}\right) \Delta c^{(0)} - m_1 m_2 h \overline{\Delta c^{(0)}} \left(\frac{u_1}{\bar{u}_1}\right), \tag{6.2a}$$

with

$$h \kappa \partial_y \delta c^{(1)} = 0 \quad \text{on} \quad y = y_L, y_R \tag{6.2b}$$

and

$$\delta c^{(1)} = -[c^{(0)}] G_+ \quad \text{at} \quad x = x_0. \tag{6.2c}$$

In order to improve upon (5.1), what we need to know is the value of the integral

$$2 \int_{x_0}^{x} \frac{\overline{\delta c^{(1)}}}{\bar{u}_1} \mathrm{d}x'. \tag{6.3}$$

Again we follow the prescription given in Appendix A with

$$a(x,y) = \delta c^{(1)}, \quad M(x,y) = \Delta c^{(0)}\left(1-\frac{u_1}{\bar{u}_1}\right), \quad N(x,y) = 1. \tag{6.4}$$

Hence once more the appropriate upstream function is $G_-(x,y)$ (4.3)), and (A 8) yields

$$\int_{x_0}^{x} \frac{\overline{\delta c^{(1)}}}{\bar{u}_1}\,\mathrm{d}x' = \int_{x_0}^{x} \frac{\overline{\Delta c^{(0)}\left(1-\frac{u_1}{\bar{u}_1}\right)G_-}}{\bar{u}_1}\,\mathrm{d}x' - [\delta c^{(1)} G_-] - [c^{(0)}][G_+ G_-]_{x_0}. \tag{6.5}$$

What has been gained is that an integral involving $\delta c^{(1)}$ has been replaced by an integral involving $\Delta c^{(0)}$ (i.e. one step down the hierarchy of moments).

We repeat the use of the prescription, but now with

$$a(x,y) = \Delta c^{(0)}, \quad M(x,y) = 0, \quad N(x,y) = \left(1-\frac{u_1}{\bar{u}_1}\right)G_-. \tag{6.6}$$

Thus we define a new auxiliary function $G_-^{(2)}(x,y)$ which satisfies the upstream advection–diffusion equation

$$-m_1 m_2 h u_1 \partial_x G_-^{(2)} - \partial_y\left(\frac{m_1}{m_2} h\kappa\, \partial_y G_-^{(2)}\right) = -m_1 m_2 h \bar{G}_-\left(\frac{u_1}{\bar{u}_1}\right) + m_1 m_2 h\left(1-\frac{u_1}{\bar{u}_1}\right)G_-, \tag{6.7a}$$

with

$$h\kappa\, \partial_y G_-^{(2)} = 0 \quad \text{on} \quad y = y_{\mathrm{L}}, y_{\mathrm{R}}, \tag{6.7b}$$

and

$$[G_-^{(2)}] = 0. \tag{6.7c}$$

This time (A 8) yields

$$\int_{x_0}^{x} \frac{\overline{\Delta c^{(0)}\left(1-\frac{u_1}{\bar{u}_1}\right)G_-}}{\bar{u}_1}\,\mathrm{d}x' = \left(\frac{\overline{qG_-^{(2)}}}{\bar{u}_1}\right)_{x_0} - [\Delta c^{(0)} G_-^{(2)}]. \tag{6.8}$$

Combining together the results (6.1), (6.5), (6.8), we find that (2.12) with $j = 2$ yields the exact expression

$$[c^{(2)}] = 2[c^{(0)}]\left\{\int_{x_0}^{x} \frac{\bar{G}_+}{\bar{u}_1}\,\mathrm{d}x' - [G_+ G_-]_{x_0} + \left(\frac{qG_-^{(2)}}{\bar{q}}\right)_{x_0}\right\} - 2[\delta c^{(1)} G_-] - 2[\Delta c^{(0)} G_-^{(2)}]. \tag{6.9}$$

At large distances downstream the last two terms tend to zero. Thus the amended asymptotic expansion (5.3) for the temporal variance is

$$\Sigma_T^2 \sim 2\int_{x_0}^{x} \frac{\bar{G}_+}{\bar{u}_1}\,\mathrm{d}x' - 2[G_+ G_-]_{x_0} + 2\left(\frac{\overline{qG_-^{(2)}}}{\bar{q}}\right)_{x_0} - \left(\frac{\overline{qG_-}}{\bar{q}}\right)^2_{x_0}. \tag{6.10}$$

To compare the relative impacts of different discharge profiles $q(y_0)$ upon the concentration experienced far downstream, it suffices to evaluate the two auxiliary functions $G_-(x,y)$, $G_-^{(2)}(x,y)$ (see figure 3). In (6.10) the $-2[G_+ G_-]$ term tends to make the variance be less (and the concentrations higher) than the dispersion-coefficient prediction

$$2\int_{x_0}^{x} \frac{D_{\mathrm{loc}}}{\bar{u}_1^3}\,\mathrm{d}x' \tag{6.11}$$

(Smith 1983). The negative contribution to Σ_T^2 can be attributed to the initial inefficiency of the shear-dispersion process close to the discharge (see figure 4). For the spatial moments Chatwin (1970, equation 4.9) was the first to quantify this deficit variance. Its influence upon the concentration only decays as the square root of time or of distance downstream.

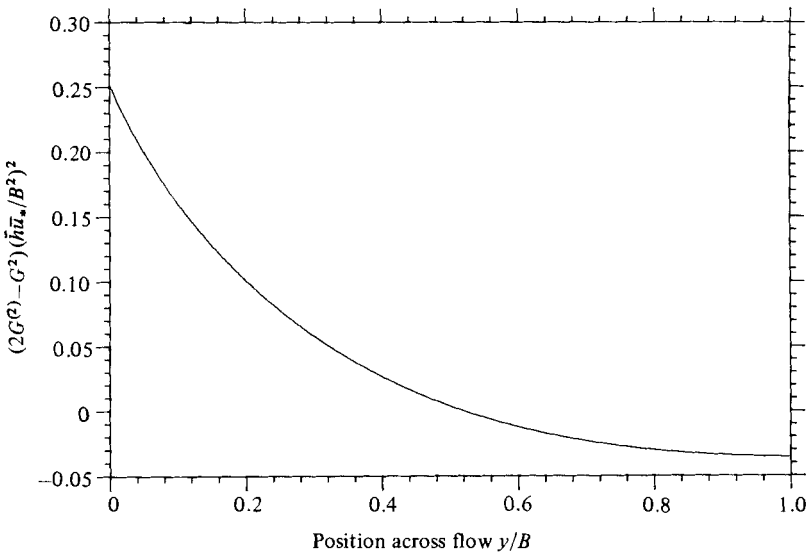

FIGURE 3. Temporal variance contribution $2G_-^{(2)}-G_-^2$ for a point discharge in a longitudinally uniform channel of triangular cross-section.

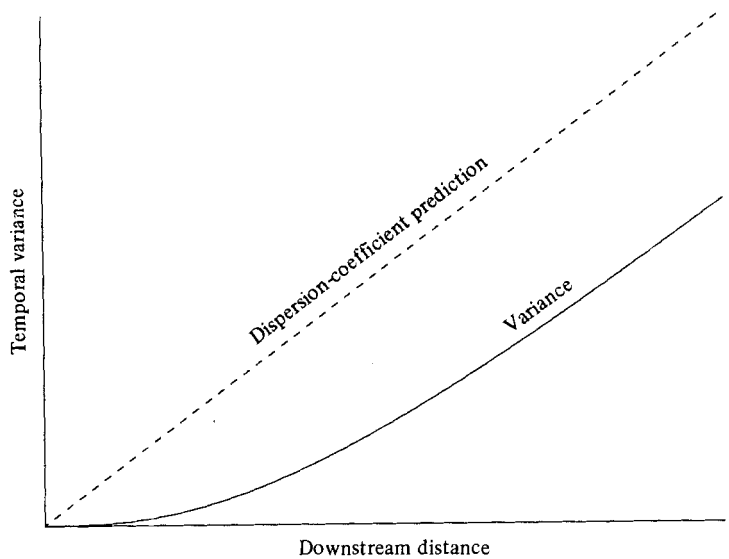

FIGURE 4. Sketch of the x-dependence of the temporal variance, showing the initial inefficiency and eventual linear growth rate with distance.

7. Importance of the monitoring position on the pollution level

Using the decomposition (6.1) for $\Delta c^{(1)}$, and the solution (4.4) for $[c^{(1)}]$, we find that the advection–diffusion equation for $\Delta c^{(2)}$ takes the form

$$m_1 m_2 h u_1 \partial_x \Delta c^{(2)} - \partial_y\left(\frac{m_1}{m_2} h\kappa\, \partial_y \Delta c^{(2)}\right)$$
$$= [c^{(0)}]\, 2m_1 m_2 h\left\{\left(\frac{\overline{qG_-}}{\bar{q}}\right)_{x_0}\left(1-\frac{u_1}{\bar{u}_1}\right)-\frac{u_1}{\bar{u}_1}\bar{G}_+ +\left(1-\frac{u_1}{\bar{u}_1}\right)G_+\right\}$$
$$+2m_1 m_2 h\left\{-\left(1-\frac{u_1}{\bar{u}_1}\right)[G_-\,\Delta c^{(0)}]-\frac{u_1}{\bar{u}_1}\overline{\delta c^{(1)}}+\left(1-\frac{u_1}{\bar{u}_1}\right)\delta c^{(1)}\right\}, \qquad (7.1a)$$

with

$$hK\partial_y \Delta c^{(2)} = 0 \quad \text{on} \quad y = y_L, y_R \tag{7.1b}$$

and

$$\Delta c^{(2)} = 0 \quad \text{at} \quad x = x_0. \tag{7.1c}$$

At large distance downstream the $\Delta c^{(0)}$ and $\delta c^{(1)}$ forcing terms vanish. Thus we have the asymptote

$$\Delta c^{(2)} \sim 2[c^{(0)}]\left(\frac{\overline{qG_-}}{\bar{q}}\right)_{x_0} G_+ + 2[c^{(0)}]G_+^{(2)}, \tag{7.2}$$

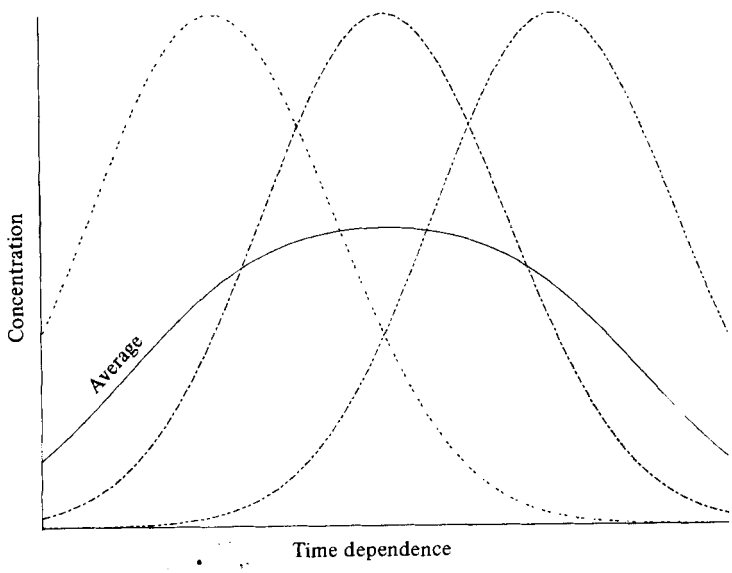

FIGURE 5. An illustration that averaging introduces additional spreading (and reduces the peak).

where the auxiliary function $G_+^{(2)}$ satisfies the downstream advection–diffusion equation (cf. the equation (6.7) for $G_-^{(2)}$):

$$m_1 m_2 h u_1 \partial_x G_+^{(2)} - \partial_y\left(\frac{m_1}{m_2} hK \partial_y G_+^{(2)}\right) = m_1 m_2 h\left(1 - \frac{u_1}{\bar{u}_1}\right) G_+ - m_1 m_2 h\left(\frac{u_1}{\bar{u}_1}\right)\bar{G}_+, \tag{7.3a}$$

with

$$hK\partial_y G_+^{(2)} = 0 \quad \text{on} \quad y = y_L, y_R, \tag{7.3b}$$

and

$$[G_+^{(2)}] = 0. \tag{7.3c}$$

The corresponding asymptotic result for the temporal variance at the location (x, y) is

$$\sigma_T^2(x,y) = \frac{c^{(2)}}{c^{(0)}} - \left(\frac{c^{(1)}}{c^{(0)}}\right)^2$$

$$\sim 2\int_{x_0}^{x} \frac{\bar{G}_+}{\bar{u}_1} dx' - 2[G_+ G_-]_{x_0} + 2\left(\frac{\overline{qG_-^{(2)}}}{\bar{q}}\right)_{x_0} - \left(\frac{\overline{qG_-}}{\bar{q}}\right)_{x_0}^2 + 2G_+^{(2)}(x,y) - G_+(x,y)^2. \tag{7.4}$$

For a point discharge at the position (x_0, y_0) there is an obvious symmetry between the dependence of the temporal variance σ_T^2 upon the observation and discharge positions (see (9.2) below). In view of the comments at the beginning of §6 concerning

the magnitude of the discharge effect, the precise monitoring position is correspondingly important. As a general rule, the lowest pollution levels can be expected when the monitoring (or freshwater extraction) takes place near the bank (Smith 1981; Daish 1984).

It deserves note that the flux-weighted average $-[G_+^2]$ of the final term in the above expression (7.4) is strictly negative. Thus the variance Σ_T^2 of the flux-averaged concentration given by (6.10) is larger than the non-averaged variance σ_T^2 (see figure 5). However, the q-dependence is precisely the same for both Σ_T^2 and σ_T^2.

8. An alternative definition of the shear-dispersion coefficient

The definition (5.4) of the shear-dispersion coefficient $D_{\rm loc}$ is based upon the variance Σ_T^2 of the flux-averaged concentration $[c]$. The purpose of this section is to give an alternative definition. $\tilde{D}_{\rm loc}$ based upon the flux average of the y-dependent variance σ_T^2. The relationship between $D_{\rm loc}$ and $\tilde{D}_{\rm loc}$ gives us insight into the occurrence of negative values of $D_{\rm loc}$ (Fukuoka & Sayre 1973).

Starting from the result (7.4), we make use of the equations (4.8), (7.3) satisfied by G_+, $G_+^{(2)}$ to derive the advection–diffusion equation

$$m_1 m_2 h u_1 \partial_x \sigma_T^2 - \partial_y \left(\frac{m_1}{m_2} h\kappa \partial_y \sigma_T^2 \right) \sim 2 \frac{m_1}{m_2} h\kappa (\partial_y G_+)^2, \tag{8.1a}$$

with

$$h\kappa \partial_y \sigma_T^2 = 0 \quad \text{on} \quad y = y_{\rm L}, y_{\rm R}. \tag{8.1b}$$

The strict positiveness of the right-hand-side forcing term in (8.1a) implies that there is a general tendency for σ_T^2 to grow downstream. Indeed, integrating (8.1a) across the flow, we have

$$\partial_x [\sigma_T^2] \sim 2 \frac{\tilde{D}_{\rm loc}}{\bar{u}_1^3}, \tag{8.2a}$$

with

$$\frac{\tilde{D}_{\rm loc}}{\bar{u}_1^2} = \overline{\frac{\kappa}{m_2^2} (\partial_y G_+)^2}, \tag{8.2b}$$

where $\tilde{D}_{\rm loc}$ is always positive.

From the equation (4.8) satisfied by G_+ we can deduce that the alternative definitions (5.4), (8.2b) of the local shear-dispersion coefficient are related:

$$D_{\rm loc} = \tilde{D}_{\rm loc} + \tfrac{1}{2} \bar{u}_1^3 \partial_x [G_+^2]. \tag{8.3}$$

Thus the condition for $D_{\rm loc}$ to become negative is that $[G_+^2]$ should strongly decrease downstream. What this means is that on average the displaced time of arrival $G_+(x, y)$ at different stations across the flow should suddenly reduce. Instead of the contaminant peaks for different values of y being widely spread out, the contaminant peaks all arrive at very much the same time (see figure 5), yielding a higher averaged concentration.

At extremely large distances downstream the dispersion coefficient predictions

$$\Sigma_T^2 \sim 2 \int_{x_0}^{x} \frac{D_{\rm loc}}{\bar{u}_1^3} \, {\rm d}x', \tag{8.4a}$$

$$[\sigma_T^2] \sim 2 \int_{x_0}^{x} \frac{\tilde{D}_{\rm loc}}{\bar{u}_1^3} \, {\rm d}x' \tag{8.4b}$$

agree to within the order of the correction terms given in (6.10), (7.4). So, at large enough distances, the choice of definition eventually becomes unimportant.

We remark that the positivity of the cross-sectionally averaged growth rate $\partial_x[\sigma_T^2]$ does not imply a universal property for all x, y. Cross-stream diffusion of σ_T^2 (see (8.1a)) out of a region of high σ_T^2 can locally give a downstream decrease in σ_T^2, and hence an increase in concentration along a streamline. Equivalently, if the shear-dispersion process had been comparatively efficient along a particular streamline, then the concentration would be low and diffusion from adjacent streamlines could increase the concentration. Hence, just as there can exist optimal discharge sites, there can be optimal extraction sites where the water has a minimum pollution level as compared with all nearby sites – even those slightly downstream.

9. Point discharges

If the discharge has the form

$$m_1 m_2 hq = \bar{q}\delta(y-y_0)\int_{y_R}^{y_L} m_1 m_2 h\,\mathrm{d}y', \tag{9.1}$$

then the asymptotic expansion (7.4) for the temporal variance σ_T^2 becomes

$$\sigma_T^2 \sim 2\int_{x_0}^{a}\frac{\bar{G}_-}{\bar{u}_1}\mathrm{d}x' + 2G_-^{(2)}(x_0,y_0) - G_-(x_0,y_0)^2 + 2\int_a^x \frac{\bar{G}_+}{\bar{u}_1}\mathrm{d}x' + 2G_+^{(2)}(x,y) - G_+(x,y)^2 - 2[G_+G_-]_a. \tag{9.2}$$

Upstream of the arbitrary reference position $x = a$, we have made use of the result (4.11) to eliminate $\bar{G}_+$ in favour of $\bar{G}_-$. It is now straightforward to reverse the roles of the discharge and observation positions, and to ask for a fixed monitoring position (x, y) how does the temporal variance depend upon the choice of discharge site (x_0, y_0). As was noted at the end of §7, when investigating the relative performance of different discharge sites Σ_T^2 and σ_T^2 can be used interchangeably.

Making use of the equations (4.3), (6.7) satisfied by G_- and $G_-^{(2)}$, we obtain the upstream counterpart of (8.1):

$$-m_1 m_2 h u_1 \frac{\partial}{\partial x_0}\sigma_T^2 - \frac{\partial}{\partial y_0}\left(\frac{m_1}{m_2}h\kappa\frac{\partial}{\partial y_0}\sigma_T^2\right) = 2\frac{m_1}{m_2}h\kappa\left(\frac{\partial G_-}{\partial y_0}\right)^2, \tag{9.3a}$$

with

$$h\kappa\frac{\partial\sigma_T^2}{\partial y_0} = 0 \quad \text{on} \quad y_0 = y_L, y_R, \tag{9.3b}$$

where the coefficients $m_1, m_2, u_1, \kappa, G_-$ are all to be evaluated at the discharge position (x_0, y_0).

As argued in §8, the strict positiveness of the forcing term in (9.3a) implies that there is an overall tendency for σ_T^2 to grow upstream with respect to x_0. Thus, in accord with physical intuition, displacing the discharge further upstream gives more time for contaminant dispersion, and tends to reduce the concentrations experienced far downstream.

Again we emphasize that the negativeness of $\partial[\sigma_T^2]/\partial x_0$ (integrated with respect to y_0) does not imply a universal property for all y_0. For a sufficiently severe change in flow conditions, an upstream displacement can actually reduce σ_T^2 (or equivalently

Σ_T^2). In such a circumstance there is an optimal site for a point discharge such that small displacements in any direction necessarily increase the concentration at all positions far downstream (see §12 below).

10. Skewness

Substituting the asymptotic result (7.2) into (2.12) with $j = 3$, we have

$$[c^{(3)}] \sim 6[c^{(0)}]\left(\frac{\overline{qG_-}}{\bar{q}}\right)_{x_0}\int_{x_0}^{x}\frac{\bar{G}_+}{\bar{u}_1}\,\mathrm{d}x' + 6[c^{(0)}]\int_{x_0}^{x}\frac{\overline{G_+^{(2)}}}{\bar{u}_1}\,\mathrm{d}x' + \text{constant}, \tag{10.1}$$

where the constant is associated with transient $\overline{\Delta c^{(2)}}$ contributions.

The skew coefficient Γ for the weighted-average concentration $[c]$ is defined

$$\Gamma = \left\{\frac{[c^{(3)}]}{[c^{(0)}]} - 3\frac{[c^{(1)}][c^{(2)}]}{[c^{(0)}]^2} + 2\frac{[c^{(1)}]^3}{[c^{(0)}]^3}\right\}\Big/\{\Sigma_T^2\}^{\frac{3}{2}}. \tag{10.2}$$

Thus, using the above results (4.4), (5.1), (10.1), we find that Γ has the asymptote

$$\Gamma \sim 6\int_{x_0}^{x}\frac{\overline{G_+^{(2)}}}{\bar{u}_1}\,\mathrm{d}x'\Big/\left\{2\int_{x_0}^{x}\frac{\bar{G}_+}{\bar{u}_1}\,\mathrm{d}x'\right\}^{\frac{3}{2}}. \tag{10.3}$$

Hence in a longitudinally uniform channel the decay of the skewness is at the slow rate $(x-x_0)^{-\frac{1}{2}}$ (Tsai & Holley 1978, figure 12).

Using the formula (A 8) given in Appendix A, with

$$a(x,y) = G_+^{(2)}, \quad b(x,y) = G_-, \quad M = \left(1-\frac{u_1}{\bar{u}_1}\right)G_+, \quad N = 1, \tag{10.4}$$

we can replace the $G_+^{(2)}$ integral by one involving the product G_+G_-:

$$\Gamma \sim 6\int_{x_0}^{x}\left(\frac{\overline{(1-u_1/\bar{u}_1)G_+G_-}}{\bar{u}_1}\right)\mathrm{d}x'\Big/\left\{2\int_{x_0}^{x}\left(\frac{\bar{G}_+}{\bar{u}_1}\right)\mathrm{d}x'\right\}^{\frac{3}{2}}. \tag{10.5}$$

The constraints

$$[G_+] = [G_-] = 0 \tag{10.6}$$

upon the auxiliary functions G_+, G_- imply that they will tend to be largest in magnitude where the velocity is low. This suggests that the integral $\overline{(1-u_1/\bar{u}_1)G_+G_-}$ is positive, and hence that the temporal skewness is positive (Nordin & Troutman 1980). By contrast, spatial skewness can be positive (Aris 1956, equation 27) or negative (Jayaraj & Subramanian 1978, figures 3, 4). The anomalous case of positive spatial skewness arises if there is a small region of high-speed low-shear fluid which induces a forward tail to the concentration distribution.

11. Uniform channels

For a longitudinally uniform channel (with $m_1 = 1$), temporal and spatial moments provide alternative descriptions of the same concentration distribution $c(x, y, t)$. Thus, in this limiting case, the new temporal results for varying channels should be closely related to the known results for the spatial moments. With the odd moments we can expect a sign reversal between the temporal and spatial results (a late arrival corresponds to an upstream displacement).

In axes moving with the bulk velocity $\bar{u}$, the spatial centroid is displaced by an amount (Aris 1956, equation 24):

$$X \sim \frac{\overline{qg}}{\bar{q}} + g(y) \quad \text{as} \quad t \to \infty, \tag{11.1}$$

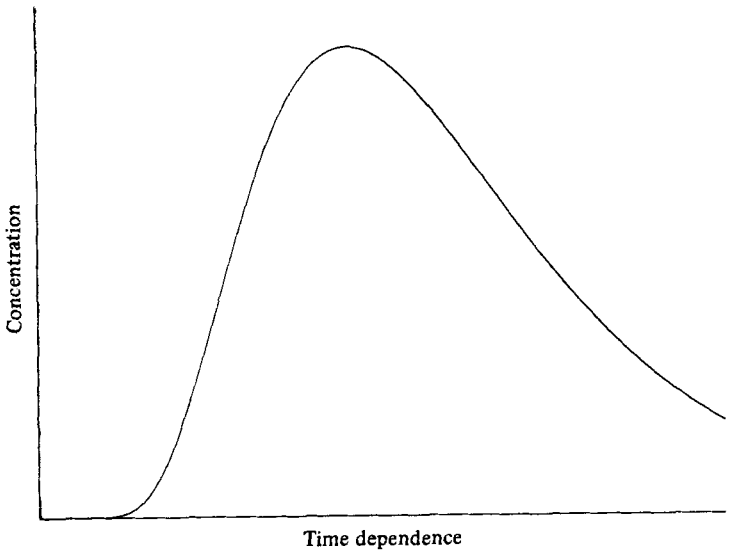

FIGURE 6. Sketch of the concentration at a fixed location as a function of time showing the rapid growth and slow decay.

where the shape function $g(y)$ satisfies the transverse diffusion equation

$$\partial_y\left(\frac{hK}{m_2}\partial_y g\right) = m_2 h(\bar{u}-u), \tag{11.2a}$$

with

$$hK\partial_y g = 0 \quad \text{on} \quad y = y_L, y_R \tag{11.2b}$$

and

$$\bar{g} = 0 \tag{11.2c}$$

(Aris 1956, equation (39); Chatwin 1970, equation (1.10); Smith 1981, equation (4.2)). The formulae connecting the two functions g, G_- are

$$G_- = \frac{\overline{ug} - \bar{u}\bar{g}}{\bar{u}^2}, \quad g = \bar{u}(\bar{G}_- - G_-). \tag{11.3}$$

Of course, for longitudinally uniform channels, there is no distinction between upstream and downstream functions, i.e. $G_+ = G_-$.

As noted by Tsai & Holley (1978), there is a systematic discrepancy between this result (11.1) for the spatial centroid and the formula

$$\bar{u}T = \bar{u}\left(\frac{\overline{qG_-}}{\bar{q}} + G_+\right) = 2\frac{\overline{ug}}{\bar{u}} - \frac{\overline{qg}}{\bar{q}} - g(y) \quad \text{as} \quad (x - x_0) \to \infty \tag{11.4}$$

for the temporal centroid. The difference (other than the obvious sign reversal) can be attributed to the fact that as the contaminant passes by the fixed location it is being continually dispersed. Thus there will be a relatively rapid increase in

concentration followed by a much slower decay (see figure 6). It is this tail which gives rise to the positive shift $2\overline{ug}/\bar{u}$ of the temporal centroid, to increased temporal variance, and to the positive temporal skewness (Chatwin 1980, equation 14).

The spatial variance for the flux-averaged concentration is given by

$$\Sigma_X^2 \sim 2\overline{ug}t - 2\overline{g^2} + 2\frac{\overline{g^{(2)}q}}{\bar{q}} - \left(\frac{\overline{gq}}{\bar{q}}\right)^2 \quad \text{as} \quad t \to \infty \tag{11.5}$$

(Smith 1981, equation 4.10). The auxiliary function $g^{(2)}$ satisfies the equation

$$\partial_y\left(\frac{h\kappa}{m_2}\partial_y g^{(2)}\right) = m_2 h\{\overline{ug} - (u-\bar{u})g\}, \tag{11.6a}$$

with

$$h\kappa\partial_y g^{(2)} = 0 \quad \text{on} \quad y = y_L, y_R \tag{11.6b}$$

and

$$\overline{g^{(2)}} = 0 \tag{11.6c}$$

(Chatwin 1970, equation 2.12). The formulae connecting the functions $g^{(2)}$ and $G_-^{(2)} = G_+^{(2)}$ are

$$G_-^{(2)} = \frac{\bar{u}g^{(2)} - \overline{(u-\bar{u})g^2}}{\bar{u}^3} + \frac{2(\overline{ug} - \bar{u}g)\,\overline{ug}}{\bar{u}^4}, \tag{11.7a}$$

$$g^{(2)} = \bar{u}^2(G_+^{(2)} - \overline{G_+^{(2)}}) - 2(G_+ - \bar{G}_+)\,\overline{ug}. \tag{11.7b}$$

From equation (4.16) of Smith (1982), we infer that at a position y across the flow the spatial variance is given by

$$\sigma_X^2 \sim \left\{2\overline{ug}t - 2\overline{g^2} + 2\frac{\overline{g^{(2)}q}}{\bar{q}} + 2g^{(2)} - g^2 - \left(\frac{\overline{gq}}{\bar{q}}\right)^2\right\} - 2\frac{\overline{gq}}{\bar{q}}g. \tag{11.8}$$

In terms of g, $g^{(2)}$, the corresponding temporal result (7.4) can be written

$$\bar{u}^2\sigma_T^2 \sim \left\{2\frac{\overline{ug}(x-x_0)}{\bar{u}} - 2\overline{g^2} + 2\frac{\overline{g^{(2)}q}}{\bar{q}} + 2g^{(2)} - g^2 - \left(\frac{\overline{gq}}{\bar{q}}\right)^2\right\}$$
$$+ 8\frac{(\overline{ug})^2}{\bar{u}^2} - 6\frac{\overline{(u-\bar{u})g^2}}{\bar{u}} - 2\frac{\overline{ug}\,\overline{gq}}{\bar{u}\bar{q}} - 2\frac{g\overline{ug}}{\bar{u}}. \tag{11.9}$$

If we make the natural identification

$$\bar{u}t = x - x_0 - \left(g + \frac{\overline{gq}}{\bar{q}}\right), \tag{11.10}$$

then far downstream the temporal variance (11.9) exceeds the spatial variance (11.8) by an amount

$$\frac{8(\overline{ug})^2}{\bar{u}^2} - \frac{6\overline{(u-\bar{u})g^2}}{\bar{u}}. \tag{11.11}$$

The leading term $8(\overline{ug})^2/\bar{u}^2$ is in agreement with the one-dimensional diffusion calculation presented by Chatwin (1980, equation 14). The second term can be attributed to the effect of the persistent spatial skewness upon the temporal variance, e.g. negative spatial skewness with a drawn-out tail makes the temporal variance larger. Remarkably, Tsai & Holley (1980) were able to obtain the coefficient of 6 with an accuracy of 1 % from their numerical solutions of the moment equations.

The spatial skewness has the asymptote

$$\gamma \sim \frac{6\overline{(u-\bar{u})\,g^2}}{(2\overline{ug})^{\frac{3}{2}}\,t^{\frac{1}{2}}} \tag{11.12}$$

(Chatwin 1970, equation 3.7), and can have either sign. From (10.5), (11.3), (11.7a), we find that at large distances downstream the temporal skewness is given by

$$\Gamma \sim 6\left\{\frac{2(\overline{ug})^2}{\bar{u}} - \overline{(u-\bar{u})\,g^2}\right\} \Big/ (2\overline{ug})^{\frac{3}{2}} \left(\frac{x-x_0}{\bar{u}}\right)^{\frac{1}{2}}. \tag{11.13}$$

The additional positive contribution to the skewness is precisely calculated by Chatwin (1980, equation 14).

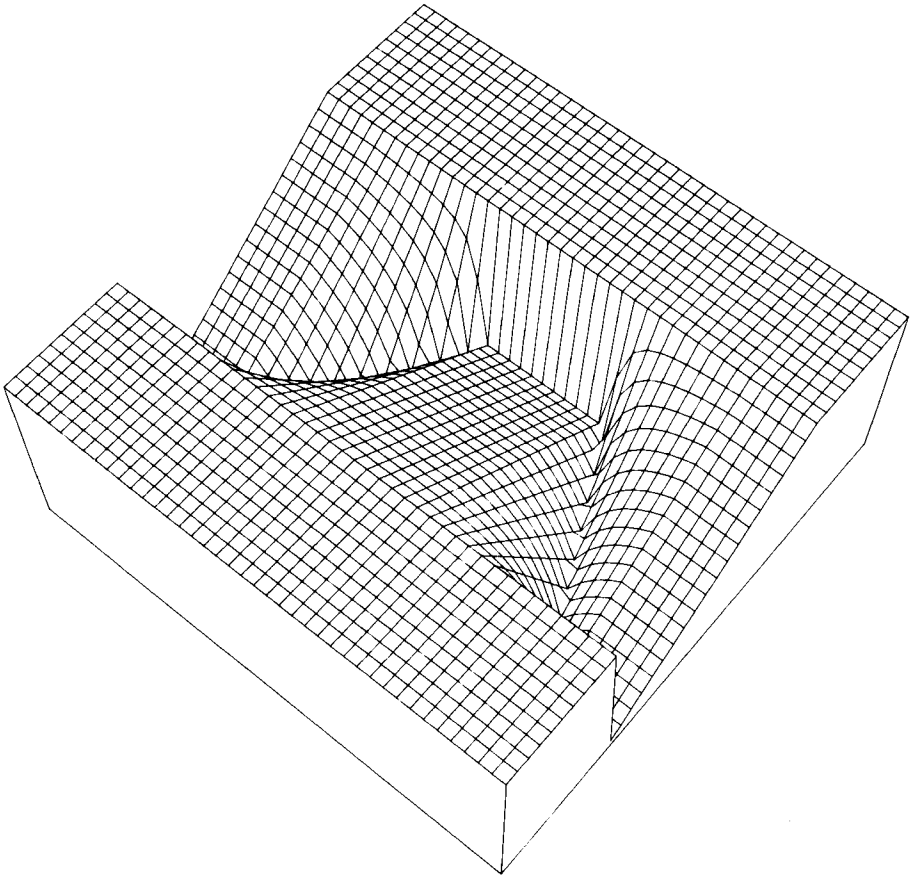

FIGURE 7. A perspective view of the depth topography, with the position of maximum depth meandering from side to side of the channel.

12. An illustrative example

In this section numerical results are given for a periodically changing depth profile, with triangular cross-section, which fairly abruptly changes in its asymmetry from one side to the other (see figure 7). To model the flow velocity u and the transverse dispersion coefficient κ we use the formulae

$$u = \frac{\bar{u}\bar{h}^{\frac{1}{2}}h}{\bar{h}^{\frac{3}{2}}}, \quad \kappa = \frac{0.15\bar{h}\bar{u}_*\,h^{\frac{3}{2}}}{\bar{h}^{\frac{3}{2}}} \tag{12.1}$$

(see Appendix B), where $\overline{u_*}$ is the area-averaged friction velocity, and the quantities $\bar{h}, \overline{h^{\frac{3}{2}}}$ are area averages *without* the usual depth weighting. The numerical factor 0.15 is based upon the experiments of Sumer (1976). The increase of u with $h^{\frac{1}{2}}$ means that in the profile transition region there is a pronounced shift of flow lines towards the deeper side (see figure 8). Despite this, we shall assume that the channel lengthscale is so much greater than the breadth scale that curvature is negligible:

$$m_1 = 1, \quad m_2 = \frac{\overline{h^{\frac{3}{2}}}}{h^{\frac{3}{2}}} f(y). \tag{12.2}$$

(For graphical convenience the figures have foreshortened longitudinal scales. Real rivers are long and narrow.)

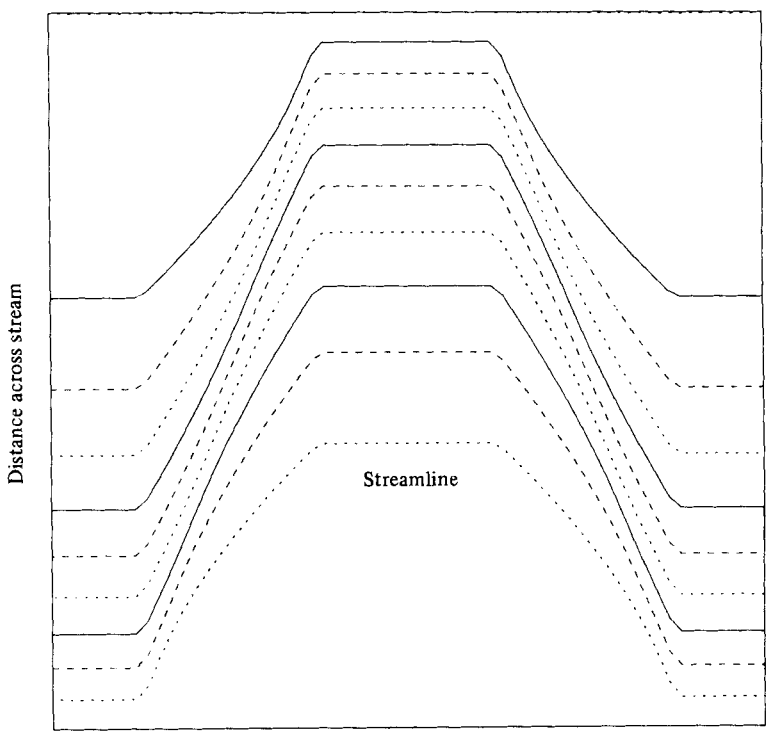

FIGURE 8. The flow lines, showing the greater separation in shallower water. The widthscale is greatly exaggerated.

Figure 9 shows contours of the time-lag function G_- over a cycle length $2L$ of the periodically changing depth profile, with

$$\frac{L\bar{h}\overline{u}_*}{B^2\bar{u}} = 1. \tag{12.3}$$

It can be seen that the discharge site needs to be well upstream of the transition region before the time lag approximates that for a longitudinally uniform channel (see figure 2). For the upstream function G_+ the contours need to be inverted horizontally.

Figure 10 shows contours of the quality

$$\left\{2\int_{x_0}^{a} \frac{\bar{G}_-}{\bar{u}_1}\,\mathrm{d}x' + 2G_-^{(2)}(x_0, y_0) - G_-(x_0, y_0)^2\right\}\frac{\bar{h}^2\overline{u}_*^2}{B^4}, \tag{12.4}$$

with the reference position $x_0 = a$ at the centre. This measures the dependence of the variance upon the siting of a point discharge (see (9.2)). Well upstream of the transition region the tilting of the contours shows that it is best to make a sudden contaminant release at the shallow bank (see figure 3). The closed contours just upstream of the transition region reveal the remarkable feature that there is an optimal discharge site. To achieve a greater contribution to the variance, the discharge would need to be moved well upstream. The optimal site can be regarded as taking as much advantage as possible of the downstream region along the shallow bank of low velocity and high shear in which the shear-dispersion process is at its most efficient.

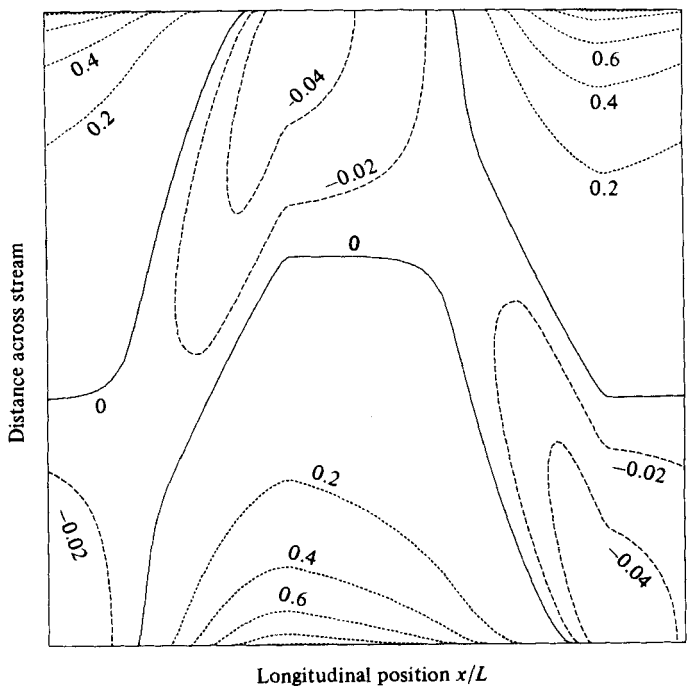

FIGURE 9. Contours of the non-dimensional time lag $G_{-}\bar{h}\bar{u}_*/B^2$ as a function of discharge position, showing the later arrival when the discharge is situated at the shallow bank.

For the dependence of the variance upon the monitoring position the appropriate measure is

$$\left\{2\int_a^x \frac{\bar{G}_+}{\bar{u}_1}\,\mathrm{d}x' + 2G_+^{(2)}(x,y) - G_+(x,y)^2\right\}\frac{\bar{h}^2\bar{u}_*^2}{B^4} \tag{12.5}$$

(see (9.2)). For the particular depth topography being studied here, the contours are the horizontal inversion of those given in figure 10. Therefore the closed contours arise just downstream of the transition region, and indicate the presence of an optimal site for the extraction of water from the river, i.e. advantage is taken of the protection afforded by the efficient dilution along the upstream region of shallow water.

We remark that there is not a worst position for water extraction (nor a worst discharge site). The diffusive character of the dispersion process ensure that as the contaminant is carried downstream the overall peak concentration decays. For each cross-section there is a constrained worst position, but there is improvement if downstream displacement is permitted. It is the shifting from side to side of the

channel of these constrained worst positions that cut off the high-σ_T^2 contours and gives rise to the existence of optimal sites.

This work was supported by the Royal Society through the award of a Research Fellowship in the Physical Sciences.

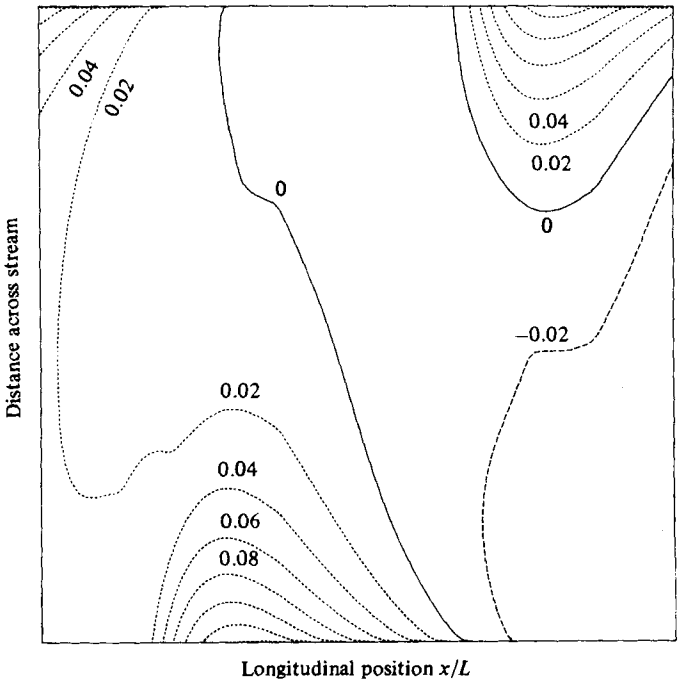

FIGURE 10. Contours of the non-dimensional contribution to the variance associated with the precise location of the contaminant release site. The optimal sites are just upstream of the stretches of shallow water.

Appendix A. Evaluation of some integrals

Consider the pair of downstream and upstream advection–diffusion equations

$$m_1 m_2 h u_1 \partial_x a - \partial_y\left(\frac{m_1}{m_2} h\kappa \partial_y a\right) = \left(M - \bar{M}\frac{u_1}{\bar{u}_1}\right) m_1 m_2 h, \tag{A 1a}$$

$$m_1 m_2 h u_1 \partial_x b + \partial_y\left(\frac{m_1}{m_2} h\kappa \partial_y b\right) = \left(\bar{N}\frac{u_1}{\bar{u}_1} - N\right) m_1 m_2 h, \tag{A 1b}$$

$$h\kappa \partial_y a = h\kappa \partial_y b = 0 \quad \text{on} \quad y = y_L, y_R. \tag{A 1c}$$

Depending upon the forcing terms M, N, the function $a(x, y)$ could be any one of $\Delta c^{(0)}$, G_+, $\delta c^{(1)}, \ldots$, while $b(x, y)$ could be G_-, $G_-^{(2)}, \ldots$.

The area averages of (A 1a), (A 1b) yield the equations

$$\partial_x[a] = \partial_x[b] = 0, \tag{A 2}$$

where the flux-weighted averages $[\ldots]$ are defined by (2.9). Thus the quantities $[a]$, $[b]$ can be evaluated at the discharge site x_0.

Multiplying (A 1 a) by $b(x,y)$, and (A 1 b) by $a(x,y)$, taking the sum and integrating across the flow, we obtain the equation

$$\bar{u}_1 \partial_x[ab] = \overline{Mb} - \overline{M}[b] + \overline{N}[a] - \overline{Na}. \tag{A 3}$$

Performing a further integration with respect to x we arrive at the result

$$\int_{x_0}^{x} \frac{\overline{Na}}{\bar{u}_1} \mathrm{d}x' = \int_{x_0}^{x} \frac{\overline{Mb}}{\bar{u}_1} \mathrm{d}x' - [b]_{x_0} \int_{x_0}^{x} \frac{\overline{M}}{\bar{u}_1} \mathrm{d}x' + [a]_{x_0} \int_{x_0}^{x} \frac{\overline{N}}{\bar{u}_1} \mathrm{d}x' - [ab] + [ab]_{x_0}. \tag{A 4}$$

Suppose, as repeatedly happens in the above analysis, we need to evaluate an integral of the form

$$\int_{x_0}^{x} \frac{\overline{Na}}{\bar{u}_1} \mathrm{d}x', \tag{A 5}$$

where $N(x,y)$ is specified (e.g. $N = 1$) and $a(x,y)$ satisfies a downstream advection–diffusion equation of the form (A 1 a). From (A 1 b) the forcing $N(x,y)$ defines an auxiliary function $b(x,y)$, where without loss of generality we can choose

$$[b] = 0. \tag{A 6}$$

Typically, the initial conditions or the forcing term in (A 1 a) are also such that

$$[a]_{x_0} = 0. \tag{A 7}$$

When all these conditions (A 6), (A 7) apply, the result (A 4) acts as a reduction formula, replacing the $\overline{Na}$-integral by the lower-order $\overline{Mb}$-integral:

$$\int_{x_0}^{x} \frac{\overline{Na}}{\bar{u}_1} \mathrm{d}x' = \int_{x_0}^{x} \frac{\overline{Mb}}{\bar{u}_1} \mathrm{d}x' + [ab]_{x_0} - [ab]. \tag{A 8}$$

If the component terms of $M(x,y)$ (e.g. $\Delta c^{(0)}$) themselves satisfy an advection–diffusion equation of the form (A 1 a), then the process can be repeated until an explicit formula is obtained.

Appendix B. The transverse shear in a shallow stream

In a shallow stream the velocity gradient, and hence the transfer of momentum, is primarily vertical. For vertical mixing (of mass or momentum) the upstream memory lengthscale is only of the order of 40 water depths. Thus in the momentum equation it is reasonable to neglect both transverse diffusion and longitudinal advection:

$$\partial_z(\nu \partial_z u) = -\partial_x p, \tag{B 1 a}$$

with

$$u = 0 \quad \text{on} \quad z = -h, \tag{B 1 b}$$

and

$$\nu \partial_z u = 0 \quad \text{on} \quad z = 0, \tag{B 1 c}$$

where ν is the eddy viscosity.

The pressure gradient $\partial_x p$ cannot vary very much across the flow, as otherwise it would drive a bulk cross-flow and the axes would be realigned accordingly. Hence we can infer from (B 1 a) that the velocity has the form

$$u = \frac{h^2}{\|\nu\|} s\left(\frac{z}{h}\right), \tag{B 2}$$

where $\|\nu\|$ is the vertically averaged eddy viscosity, and the shape function $s(z/h)$ describes the detailed velocity profile.

In constant-depth open-channel flows it has repeatedly been verified that the eddy diffusivities for momentum and for mass scale as the product hu_* of the depth h and friction velocity u_* (Elder 1959; Sumer 1976). If we assume that the upstream memory and cross-stream diffusion of the turbulence can be neglected, then this local modelling for ν enables us to modify the representation (B 2):

$$u \propto \frac{h}{u_*} s\left(\frac{z}{h}\right). \tag{B 3}$$

The turbulence is generated by the flow past the roughness elements on the bed (or by instability of the flow). This leads to proportionality between u_* and $\|u\|$, the precise ratio depending weakly upon the roughness height. Again, assuming a local response, we infer that u varies as $h^{\frac{1}{2}}$:

$$u \propto h^{\frac{1}{2}} s\left(\frac{z}{h}\right). \tag{B 4}$$

It then follows that the friction velocity u_* varies as $h^{\frac{1}{2}}$ and the eddy diffusivities ν, κ as $h^{\frac{3}{2}}$.

The weakest point in the above argument is in the neglect of cross-stream influences. Fischer (1969) showed that when there are bends the centrifugal effect leads to secondary flows which greatly augment the cross-stream diffusion of mass. Empirically this can be accounted for by increasing the coefficient 0.15 in equation (12.1) for κ. For example, the author (Smith 1983, equation 10.3) has used the formula

$$\kappa = 0.15(1 + F(x)) \frac{\bar{h}\bar{u}_* \bar{h}^{\frac{3}{2}}}{\overline{h^{\frac{3}{2}}}}, \tag{B 5}$$

where the Fischer number $F(x)$ depends upon the curvature of the channel:

$$F = 200(\bar{h}\rho)^2 \left(\frac{\bar{u}}{\bar{u}_*}\right)^2. \tag{B 6}$$

Although the radius of curvature $1/\rho$ is several orders of magnitude greater than the water depth, the large values of the factors 200 and $(\bar{u}/\bar{u}_*)^2$ can make F be of order unity.

REFERENCES

Aris, R. 1956 On the dispersion of a solute in a fluid flowing through a tube. *Proc. R. Soc. Lond.* A **235**, 67–77.

Aris, R. 1960 On the dispersion of a solute in pulsating flow through a tube. *Proc. R. Soc. Lond.* A **259**, 370–376.

Chatwin, P. C. 1970 The approach to normality of the concentration distribution of a solute in solvent flowing along a straight pipe. *J. Fluid Mech.* **43**, 321–352.

Chatwin, P. C. 1980 Presentation of longitudinal dispersion data. *J. Hydraul. Div. ASCE* **106**, 71–83.

Daish, N. C. 1984 In preparation.

Elder, J. W. 1959 The dispersion of marked fluid in turbulent shear flow. *J. Fluid Mech.* **5**, 544–560.

Fisher, H. B. 1967 The mechanics of dispersion in natural streams. *J. Hydraul. Div. ASCE* **93**, 187–216.

Fischer, H. B. 1969 The effects of bends on dispersion in streams. *Water Resources Res.* **5**, 496–506.

Fukuoka, S. & Sayre, W. W. 1973 Longitudinal dispersion in sinuous channels. *J. Hydraul. Div. ASCE* **99**, 195–217.

Jayaraj, K. & Subramanian, R. S. 1978 On relaxation phenomena in field-flow fractionation. *Sep. Sci. Tech.* **13**, 791–817.

NORDIN, C. F. & TROUTMAN, B. M. 1980 Longitudinal dispersion in rivers: the persistence of skewness in observed data. *Water Resources Res.* **16**, 123–128.

SMITH, R. 1981 The importance of discharge siting upon contaminant dispersion in narrow rivers and estuaries. *J. Fluid Mech.* **108**, 45–53.

SMITH, R. 1982 Gaussian approximation for contaminant dispersion. *Q. J. Mech. Appl. Maths* **35**, 345–366.

SMITH, R. 1983 Longitudinal dispersion coefficients for varying channels. *J. Fluid Mech.* **130**, 299–314.

SUMER, S. M. 1976 Transverse dispersion in partially stratified tidal flow. *Univ. California, Berkeley, Hydraul. Engng Lab. Rep.* WHM-20.

TAYLOR, G. I. 1953 Dispersion of soluble matter in solvent flowing slowly through a tube. *Proc. R. Soc. Lond.* A **219**, 186–203.

TSAI, Y. H. & HOLLEY, E. R. 1978 Temporal moments for longitudinal dispersion. *J. Hydraul. Div. ASCE* **104**, 1617–1634.

TSAI, Y. H. & HOLLEY, E. R. 1980 Temporal moments for longitudinal dispersion. *J. Hydraul. Div. ASCE* **106**, 2063–2066.